Determination of resonant frequency of a piezoelectric ring for generation of ultrasonic waves

Murimi Evan (Corresponding author)
Department of Mechatronic Engineering, Jomo Kenyatta University of Agriculture and Technology
P.O. Box 62000-00200, Nairobi, Kenya
Tel: +254 67 52711 E-mail: murimev@yahoo.com

Kihiu John
Department of Mechanical Engineering, Jomo Kenyatta University of Agriculture and Technology
P.O. Box 62000-00200, Nairobi, Kenya
Tel: +254 67 52711

Nyakoe George
Department of Mechatronic Engineering, Jomo Kenyatta University of Agriculture and Technology
P.O. Box 62000-00200, Nairobi, Kenya
Tel: +254 67 52711

Mutuli Stephen
Department of Mechanical Engineering, University of Nairobi
P.O. Box P.O. BOX 30197-00100, Nairobi, Kenya
Tel: +254 02 318262

Kimotho James
Department of Mechanical Engineering, Jomo Kenyatta University of Agriculture and Technology
P.O. Box 62000-00200, Nairobi, Kenya
Tel: +254 67 52711

Abstract

Ultrasound technology has become an important aspect in material handling and machining. Standing and traveling ultrasonic waves have been applied in powder transportation, feeding, dosing and supply of small amounts of powder with high quantitative accuracy and precision. Piezoelectric actuators are the most commonly used to generate the ultrasonic waves in various devices. Hence, these devices have presented a unique, economic and simple means of accurate handling of powder. This paper describes the determination of the resonant frequency of a piezoelectric ring that can be applied for generation of the ultrasonic waves. The resonant frequency is important in determining the highest amplitude of the vibration of the ring.

Keywords—piezoelectric, resonance, ultrasonic, vibration.

1. Introduction

When mechanical stresses are applied to a piezoelectric solid, voltage is produced between its surfaces. This is the piezoelectric effect. Conversely, when a voltage is applied across certain surfaces of the solid, the solid undergoes a mechanical distortion. This is the inverse piezoelectric effect. The effect is exhibited by certain crystals whose charge symmetry is disturbed, and the charge asymmetry generates a voltage across the material. Examples include quartz, Rochelle Salt and many synthetic polycrystalline ceramics, such as bariumtitanate and lead zirconate titanates (PZT) (Vishal and Fernandes, 2010). Inverse piezoelectricity can be used to generate mechanical vibrations in ultrasonic range which can be used in handling of small particles like powder in industrial processes with more accuracy and precision (Mracek and Wallaschek, 2005) (Yamada, Nakagawa and Nakamura, 1993) (Kozuka, Tuziuti and Mitome, 1998) (Nyborg, 1967).

1.1 Piezoelectric relations

The electrical behavior of an unstressed medium under the influence of an electric field is defined by the electric field strength, E and the dielectric displacement, D. Their relationship is shown in Equation 1.

$$D = \varepsilon E \tag{1}$$

Where ε is the permittivity of the medium. The mechanical behavior of the same medium at zero electric field strength is defined by two mechanical quantities namely; the stress applied, T and the strain, S. whose relationship is shown in Equation 2

$$S = sT \tag{2}$$

where s denotes the compliance of the medium (Mason, 1950).

Piezoelectricity involves the interaction between the electrical and the mechanical behavior of the medium. This interaction can be closely approximated by linear relations (Equation 3) between electrical and mechanical variables (Kocbach, 2000).

$$\left.\begin{aligned} S &= s^E T + dE \\ D &= dT + \varepsilon^T E \end{aligned}\right\} \tag{3}$$

1.2 Vibration modes of a piezoelectric ring

Considering the ring shown in Figure 1, there are three possible fundamental modes of when an electric field parallel to the poling direction is applied (Hueter and Bolt, 1955).

1) The thickness (axial) mode vibration occurs when the applied frequency is coincident with the thickness resonant frequency, f_{thk} which induces a change in thickness, $\tau \pm \Delta \tau_r$.
2) The radial mode vibration occurs when the applied frequency is coincident with the radial resonant frequency, f_{r-rad} which induces a change in the mean diameter $d_{mr} \pm \Delta d_{mr}$. The radial mode always appears as the lowest frequency as the diameter is the largest dimension.
3) The wall thickness mode $f_{r\text{-}wd}$ occurs when the frequency is coincident with the resonant frequency along the wall thickness direction, causing a change in the wall thickness $w_r \pm \Delta w_r$ (Cheng and Chan, 2001).

The thickness resonant frequency, f_{r-thk}, radial resonant frequency, f_{r-rad} and wall thickness resonant frequency, f_{r-wall} are given in Equations 4, 5 and 6 respectively.

$$f_{r-thk} = \frac{1}{2\tau_r\sqrt{\rho . s_{33}^D}} \tag{4}$$

$$f_{r-rad} = \frac{1}{\pi d_{mr}\sqrt{\rho . s_{11}^E}} \tag{5}$$

$$f_{r-wall} = \frac{1}{2\omega_r\sqrt{\rho . s_{11}^E}} \tag{6}$$

Where $d_{mr} = (d_{outer} + d_{inner})/2$ is the mean diameter, $\omega_r = (d_{outer} - d_{inner})/2$ is the mean wall thickness, ρ is the density, τ_r is the thickness of the ring, s^E_{11} is the elastic compliance at constant electric field and s^D_{33} is the elastic compliance at constant charge density (IECstandard, 1976).

The radial mode vibration has three vibrations modes. Figure 2a is the first radial mode vibrating in its direction symmetrically, called the (R,1) mode and Figure 2b is one of the non-axisymmetric modes vibrating in its radial direction asymmetrically, called the (1,1) mode. A non-axisymmetric mode has an orthogonal mode with the same form as the degenerated mode as shown in Figures 3a and 3b.

When the degenerated modes are excited by two electric signals with a phase difference of 90^o as shown in Figure 3c, a mode rotation occurs at the inner and outer circumference of the annular plate (Takano and Tomikawa, 1997).

1.3 Radial vibration of a piezoelectric ring

Axisymmetric radial vibration can be set up in a thin ceramic ring with radial poling and electrodes connected on its inner and outer surfaces (Yang, 2005), (Yang, 2006) as shown in Figure 4.

By taking R, w and h as the mean radius, width and thickness of the ring respectively and making the assumption that R >> w >> h. Furthermore, in cylindrical coordinates and the boundary conditions, Equation 7 is approximated as true throughout the ring:

$$\left.\begin{array}{c} T_{ii} \neq 0 \\ T_{ij} = 0 \text{ for } i \neq j \\ E_\theta = E_z = 0 \end{array}\right\} \quad (7)$$

Let (θ, z, r) correspond to (1, 2, 3). The radial electric field and the tangential strain are given by

$$\left.\begin{array}{c} S_{11} = S_{\theta\theta} = \dfrac{u_r}{R} \\ E_3 = E_r = -\dfrac{V}{h} \end{array}\right\} \quad (8)$$

The relevant constitutive relations are

$$\left.\begin{array}{c} S_{11} = S_{\theta\theta} = s_{11}T_{\theta\theta} + d_{31}E_r \\ D_3 = D_r = d_{31}T_{\theta\theta} + \epsilon_{33}E_r \end{array}\right\} \quad (9)$$

Which on solving give,

$$\left.\begin{array}{c} T_{\theta\theta} = \dfrac{1}{s_{11}}\dfrac{u_r}{R} - \dfrac{d_{31}}{s_{11}}E_r \\ D_r = \dfrac{d_{31}}{s_{11}}\dfrac{u_r}{R} + \bar{\epsilon}_{33}E_r \end{array}\right\} \quad (10)$$

where

$$\bar{\epsilon}_{33} = \epsilon_{33} - d_{31}^2/s_{11} \quad (11)$$

The equation of motion takes the following form (Portelles et al., 2011);

$$-\frac{T_{\theta\theta}}{R} = \rho\ddot{u}_r \quad (12)$$

Substitution of Equation 10 into Equation 12 yields;

$$-\frac{1}{s_{11}}\frac{u_r}{R^2} + \frac{d_{31}}{s_{11}R}E_r = \rho\ddot{u}_r \quad (13)$$

substituting Equation 8 in Equation 13 gives;

$$-\frac{1}{s_{11}}\frac{u_r}{R^2} - \frac{d_{31}}{s_{11}R}\frac{V}{h} = \rho\ddot{u}_r \quad (14)$$

which can be written in the form

$$\rho \ddot{u}_r + \frac{1}{s_{11}}\frac{u_r}{R^2} = -\frac{d_{31}}{s_{11}R}\frac{V}{h} \tag{15}$$

Equation 15 can be compared with the differential equation of a spring-mass system (Equation 16) with a forcing function, F (Kelly, 2000).

$$\left.\begin{array}{c} m\ddot{x} + kx = F \\ \text{whose natural frequency}, \omega^2 = \dfrac{k}{m} \end{array}\right\} \tag{16}$$

Similarly, the natural frequency of vibration of the piezoelectric ring is given as (Kirekawa, Ito and Asano, 1992),

$$\omega^2 = \frac{1}{\rho s_{11} R^2} \tag{17}$$

2. METHODOLOGY

2.1 Modeling

Finite Element Analysis is used for modeling purposes. First, the modal analysis was done in order to determine the vibration characteristics (natural frequencies and mode shapes) of the piezoelectric ring during free vibrations. It was then meshed using automatic meshes as shown in Figure 5a, and later refined using mapped face meshing and body sizing so as to arrange the elements in a regular manner as shown in

Figure 5b. The modal shape was obtained as shown in Figure 6.

2.2 Experiments

The schematic diagram for the study is shown in Figure 7. The piezoelectric ring had the electrodes connected to its faces as shown in Figure 8. Thereafter, the ring was subjected to 10V alternating current and then the deformation graph was viewed using a digital oscilloscope. The frequency of the voltage was then varied until the deformation and the voltage curves were in phase. This state indicated that the piezoelectric ring was vibrating at the resonant frequency. Two rings were used, and the velocity of vibration of the inner and the outer faces were compared.

3. RESULTS

From the modal analysis, the piezoelectric ring was found to have a natural frequency of 47.9 kHz. Additionally, from the harmonic analysis, the ratio of deformation of the inner ring edges was obtained as shown in Table I. This showed that the ratio of the deformation of the inner edges was approximately 1 at the various exciting frequencies considered implying that there was no significant variation to the deformation of the inner edges of the ring. As a result, the whole of the inner face was used during the modeling of the deformation of the whole set-up. An analysis around the resonant frequency of the piezoelectric ring was done in order to obtain the maximum velocity of vibration of the inner and outer diameter faces. Tables II and III show the results of the face displacements. From the frequency, f, of excitation and the Amplitude, A, the velocity, V, was calculated using Equation 18.

$$V = 2\pi f A \tag{18}$$

The resonant frequency of the ring was also obtained numerically using Equation 5, whereby Equation 19 gave the mean radius of the ring in Figure 1.

$$\left.\begin{aligned} R &= \frac{d_{outer} + d_{inner}}{2 \times 2} \\ &= \frac{30 + 15}{4} \\ &= 11.25 \text{ mm} \end{aligned}\right\} \tag{19}$$

From Equation 17, the natural frequency in radial mode for the ring was obtained as;

$$\left.\begin{aligned}\omega^2 &= \frac{1}{7.85\times10^3\times1.29621\times10^{-11}\times(11.25\times10^{-3})^2}\\ &= \frac{1}{1.2878\times10^{-11}}\\ &= 7.7652\times10^{10}\end{aligned}\right\} \quad (20)$$

Hence

$$\left.\begin{aligned}\omega &= \sqrt{7.7652\times10^{10}}\\ &= 2.7866\times10^{5}\,\mathrm{rad/s}\end{aligned}\right\} \quad (21)$$

The resonant frequency in radial mode, f_{r-rad} was given by

$$\left.\begin{aligned}f_{r-rad} &= \frac{\omega}{2\pi}\\ &= \frac{2.7866\times10^5}{2\pi}\\ &= 4.4350\times10^4\ \mathrm{Hz}\end{aligned}\right\} \quad (22)$$

From the experiment, the resonant frequency of the two rings was measured as 47.96 kHz and 47.99 kHz.

4. CONCLUSION

The resonant frequency of a piezoelectric ring was obtained through various methods which gave a consistent value of the resonant frequency. Finite element analysis is therefore a suitable method for modeling the ultrasonic vibrations of a piezoelectric ring. In addition, it is possible to use a piezoelectric ring under the low voltage region to produce ultrasonic waves. Therefore, the ring is a suitable method of producing ultrasonic waves economically.

References

Cheng, K.C. and Chan, H.L.W. (2001) 'Characterization of Piezoelectric Ring Used for Wire Bonding Transducer Application', Electron devices meeting, Hunghom, Kowloon, Hong Kong, 64-67.

Hueter, T.F. and Bolt, R.H. (1955) *Sonics*, John Wiley and Sons, Inc.

IECstandard (1976) *Guide to dynamic measurements of piezoelectric ceramic with high electromechanical coupling*.

Kelly, S.G. (2000) *Fundamentals of Mechanical Vibrations*, 2nd edition, McGraw-Hill Book Co.

Kirekawa, A., Ito, Y. and Asano, K. (1992) 'A study of structural control using viscoelastic material', Eathquake engineering, Tenth world conference, Balkema, Rotterdam, 2047-2054.

Kocbach, J. (2000) *Finite Element Modeling of Ultrasonic Piezoelectric Transducers*, University of Bergen, Department of Physics.

Kozuka, T., Tuziuti, T. and Mitome, H. (1998) 'Control of Position of a Particle Using a Standing Wave Field Generated by Crossing Sound Beams', Ultrasonics Symposium, IEEE , Sendai , 357–660.

Mason, W. (1950) *Piezoelectric crystals and their applications to ultrasonics*, New York: D. Van Nostrand.

Mracek, M. and Wallaschek, J. (2005) 'A system for powder transport based on piezoelectrically excited ultrasonic progressive waves', *Materials chemistry and physics*, p. 378–380.

Nyborg, W.L. (1967) 'Radiation pressure on a small rigid sphere', *Acoustical society of America*, vol. 42, no. 5, p. 947–952.

Portelles, J., Fuentes, J., Rodriguez, E.L., L. Soto, O.R., V.Garcia, Heiras, J. and Siqueiros, J. (2011) 'Piezoelectricity: Measurement of the resonant response of the radial mode at different temperatures', *Latin-American Journal of Physics Education*, vol. 5, no. 1, March, p. 129–133.

Takano, T. and Tomikawa, Y. (1997) 'Excitation of a progressive wave in a lossy ultrasonic transmission line

and an application to a powder feeding device', *Smart Materials and Structures*, vol. 7, no. 3, pp. 417-421.
Vishal, V. and Fernandes, A.P. (2010) *Piezo electricity: Powering the Future*, M.I.T. Manipal.
Yamada, K., Nakagawa, T. and Nakamura, K. (1993) 'Powder transportation by unidirectional ultrasound radiated from a pair of phase-shifted bending vibrators', Ultrasonics Symposium , dai 980, Japan, 457-461.
Yang, J. (2005) *An introduction to the theory of piezoelectricity*, Boston: Springer Science + Business Media, Inc.
Yang, J. (2006) *The Mechanics of Piezoelectric Structures*, World Scientific Publishing Co. Pte. Ltd.

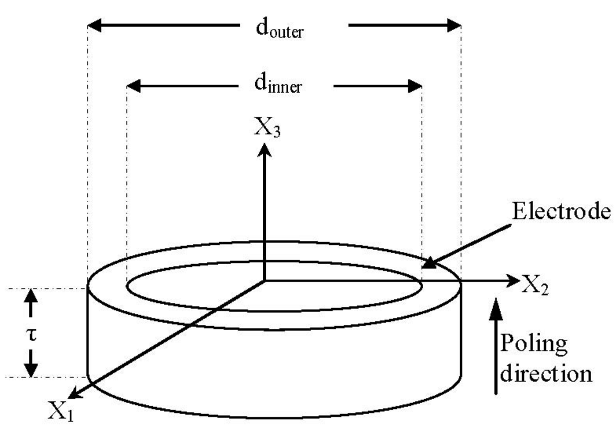

Figure 1: Schematic diagram of a piezoceramic ring.

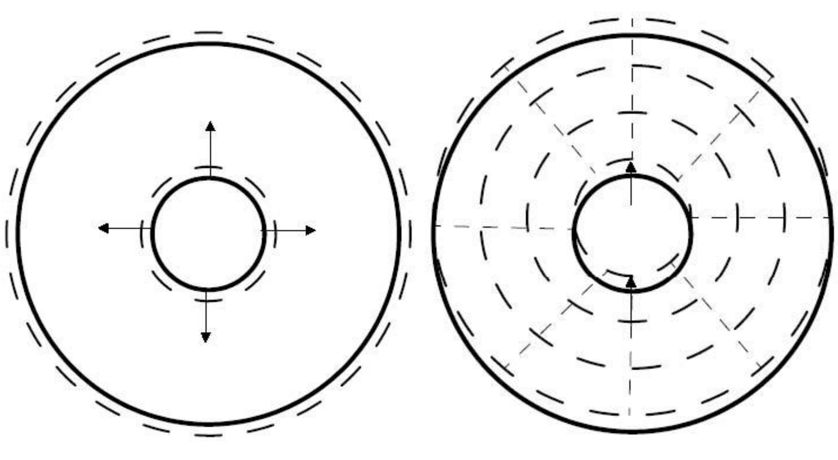

(a) (R,1) MODE (b) (1,1) MODE

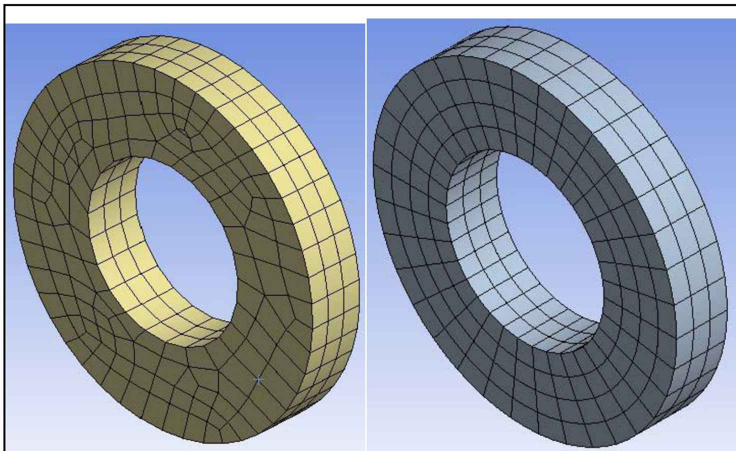

(a) Automatic meshes (b) Refined meshes

Figure 5: Mesh for the piezoelectric ring model

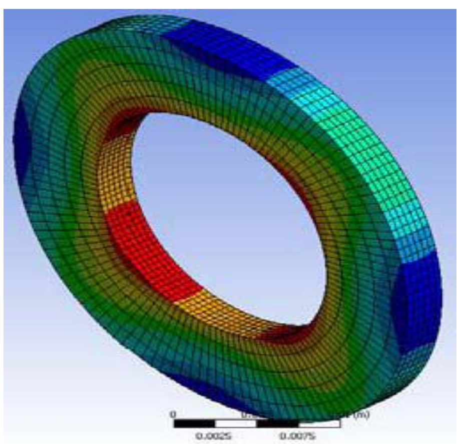

Figure 6: Modal shape for the piezoelectric ring

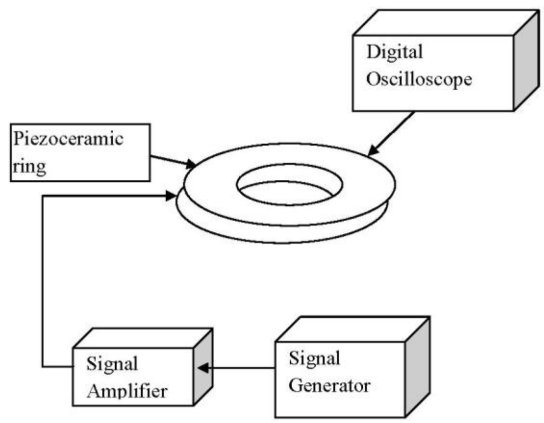

Figure 7: Schematic diagram for the experimental set-up.

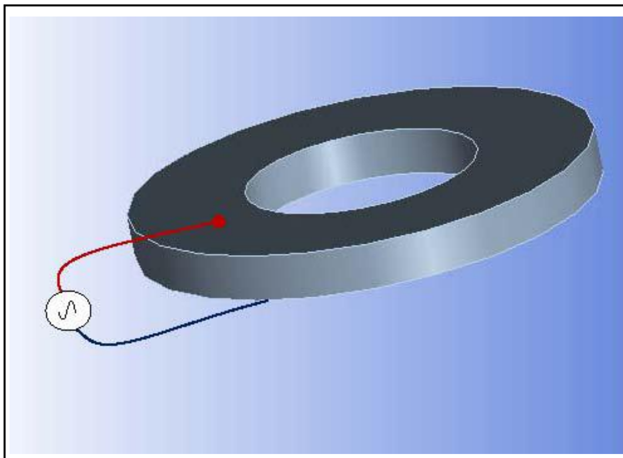

Figure 8: Electrodes connection on the piezoelectric ring.

Table 1: Deformation of the piezoelectrc inner face and edges

Offset (mm)	Amplitude at Edge 1 (m)	Amplitude at Edge 2 (m)	Amplitude Ratio
0.1	1.05E-008	1.06E-008	0.9858
1	1.05E-008	1.07E-008	0.9868
2	1.06E-008	1.07E-008	0.9894
3	1.03E-008	1.05E-008	0.9896
4	9.93E-009	9.87E-009	1.0060
5	9.97E-009	9.97E-009	1.0000
6	1.02E-008	1.01E-008	1.0124
7	1.03E-008	1.02E-008	1.0102
8	9.51E-009	9.11E-009	1.0438
9	9.39E-009	8.99E-009	1.0446
10	8.45E-009	8.22E-009	1.0282
11	9.59E-009	9.66E-009	0.9925
12	9.82E-009	9.62E-009	1.0204
13	9.91E-009	9.73E-009	1.0184
14	9.76E-009	9.50E-009	1.0274
15	9.31E-009	9.15E-009	1.0185
16	9.35E-009	9.17E-009	1.0186
17	9.66E-009	9.70E-009	0.9957
18	9.55E-009	9.58E-009	0.9971
19	9.80E-009	9.86E-009	0.9942
20	9.95E-009	9.87E-009	1.0082

Table 2: Velocity for the deformation of the inner face of the ring

Frequency (Hz)	Amplitude (m)	Velocity (mm/s)
47000	9.02E-08	2.66E+01
47200	1.02E-07	3.03E+01
47400	1.18E-07	3.51E+01
47600	1.33E-07	3.99E+01
47800	1.44E-07	4.32E+01
48000	1.45E-07	4.37E+01
48200	1.36E-07	4.11E+01
48400	1.21E-07	3.68E+01
48600	1.06E-07	3.23E+01
48800	9.22E-08	2.83E+01
49000	8.08E-08	2.49E+01

Table 3: Velocity for the deformation of the outer face of the ring

Frequency (Hz)	Amplitude (m)	Velocity (mm/s)
47000	6.99E-08	2.06E+01
47200	7.82E-08	2.32E+01
47400	8.93E-08	2.66E+01
47600	1.00E-07	3.00E+01
47800	1.74E-07	5.23E+01
48000	1.07E-07	3.23E+01
48200	9.95E-08	3.01E+01
48400	8.80E-08	2.68E+01
48600	7.62E-08	2.33E+01
48800	6.58E-08	2.02E+01
49000	5.72E-08	1.76E+01